Electronic Supplementary Material (ESI) for Polymer Chemistry.

Supporting Information

CO_2-stimulated vesicle-to-lamella transition of ABC miktoarm star terpolymer assemblies

Meng Huo[a,b], Haotian Du[a], Min Zeng[a], Long Pan[c], Tommy Fang[a], Xuming Xie[c], Yen Wei*[b] and Jinying Yuan*[a]

[a]Key Lab of Organic Optoelectronics and Molecular Engineering of Ministry of Education, Department of Chemistry, Tsinghua University, Beijing 100084, P. R. China. E-mail: yuanjy@mail.tsinghua.edu.cn

[b]Key Lab of Bioorganic Phosphorus Chemistry & Chemical Biology of Ministry of Education, Department of Chemistry, Tsinghua University, Beijing 100084, P. R. China. E-mail: weiyen@tsinghua.edu.cn

[c]Department of Chemical Engineering, Tsinghua University, Beijing 100084, P. R. China

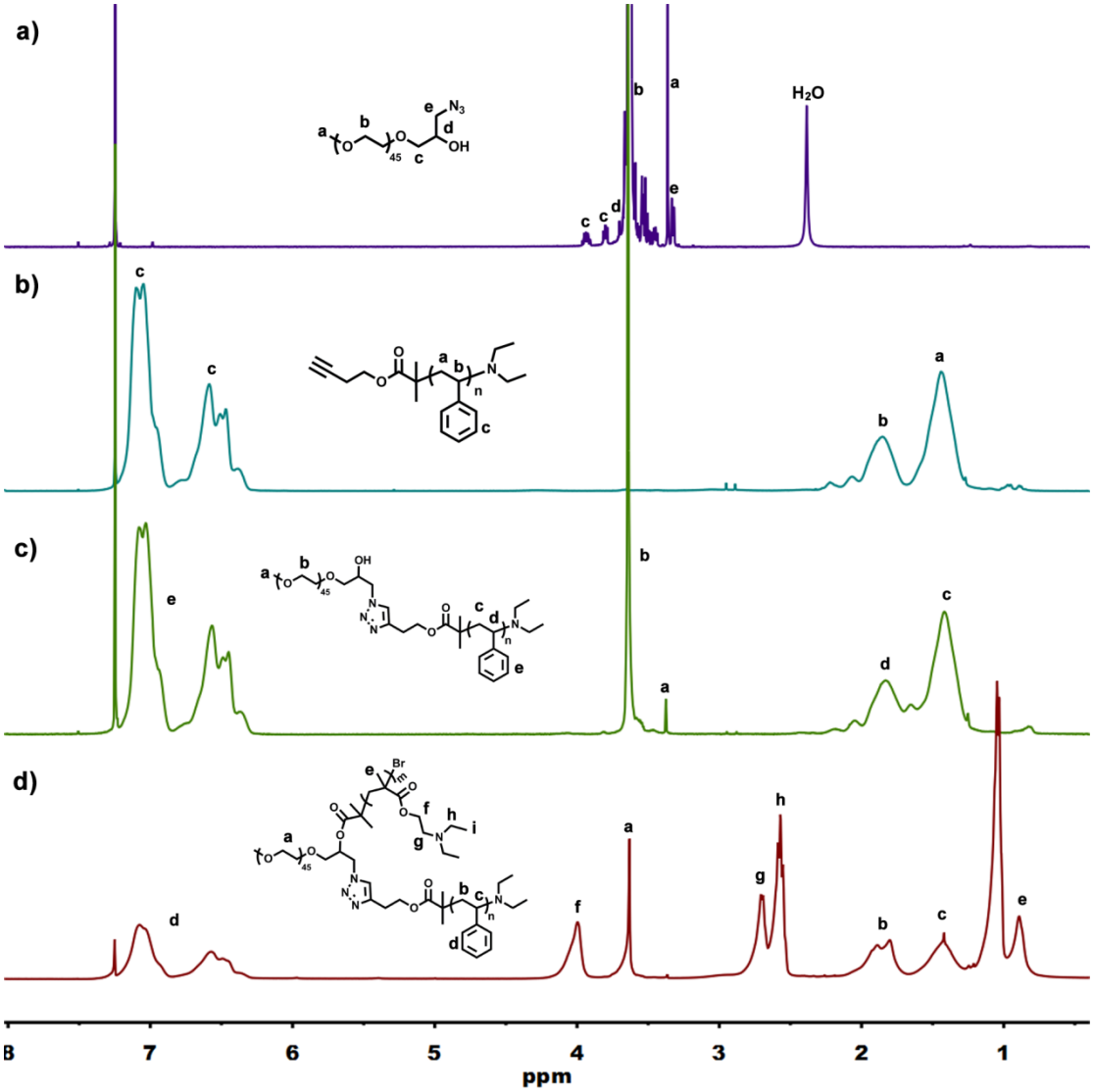

Fig. S1 ^{1}H NMR spectra of a) PEG-(OH)-N_3, b) PS-NEt_2, c) PEG-(OH)-PS, d) μ-PEG-PS-PDEA[a].

[a]The DP of PDEA was calculated using the integration of the peak a and peak f in Fig. S1d according to the following equation:

$$\mathrm{DP}_{PDEA} = \frac{45 \times 4}{2} \times \frac{I_f}{I_a}$$

where I_f represents the integration of the peak f and I_a represents the integration of the peak a.

According to the calculation the *DP*s of PDEA of μ-PEG-PS-PDEA were 18 (μ-PEG-PS-PDEA$_{3.3k}$), 37 (μ-PEG-PS-PDEA$_{6.8k}$), 50 (μ-PEG-PS-PDEA$_{9.3k}$), 66 (μ-PEG-PS-PDEA$_{12.2k}$), and 135 (μ-PEG-PS-PDEA$_{25.0k}$), respectively.

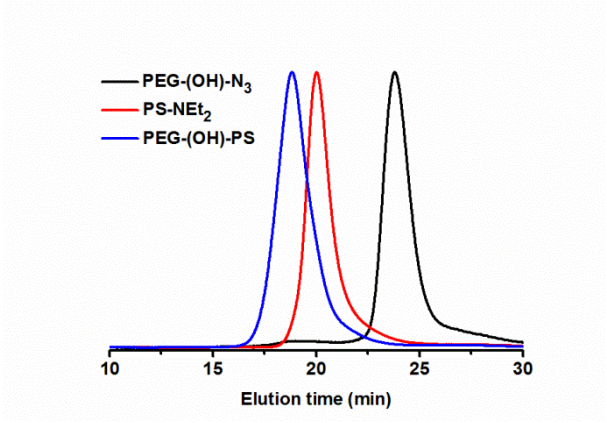

Fig. S2 GPC traces of PEG-(OH)-N_3, PS-NEt_2 and PEG-(OH)-PS.

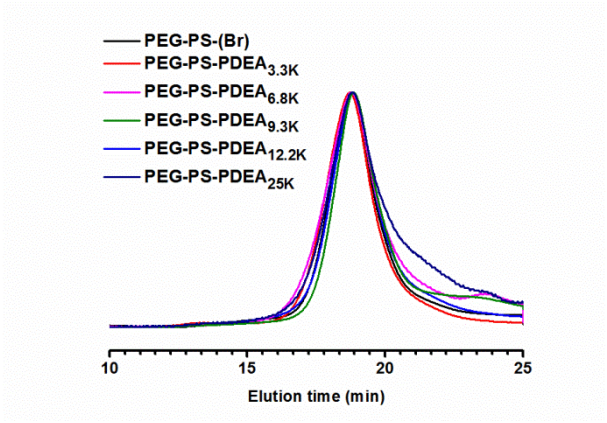

Fig. S3 GPC traces of PEG-(Br)-PS and μ-PEG-PS-PDEA with different PDEA chain lengths.

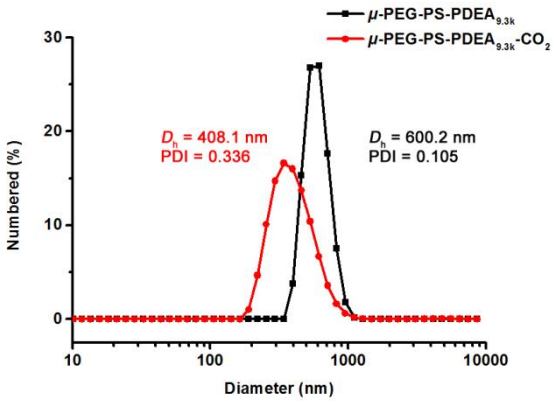

Fig. S4 DLS characterization of μ-PEG-PS-$PDEA_{9.3k}$ before and after CO_2 purging.

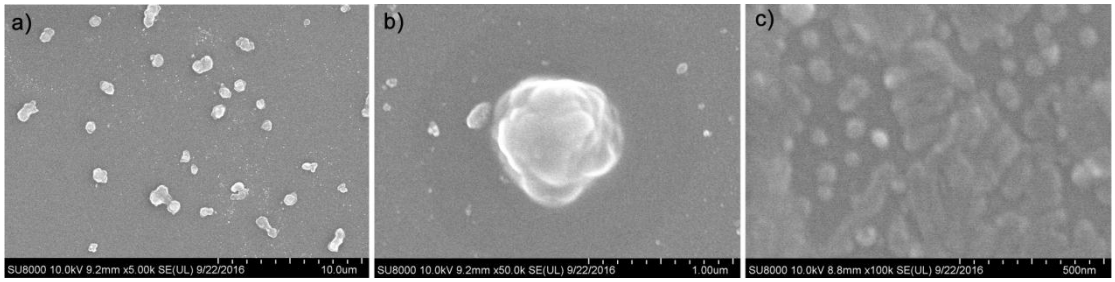

Fig. S5 SEM characterization of μ-PEG-PS-PDEA$_{9.3k}$ a), b) before and c) after CO_2 purging.

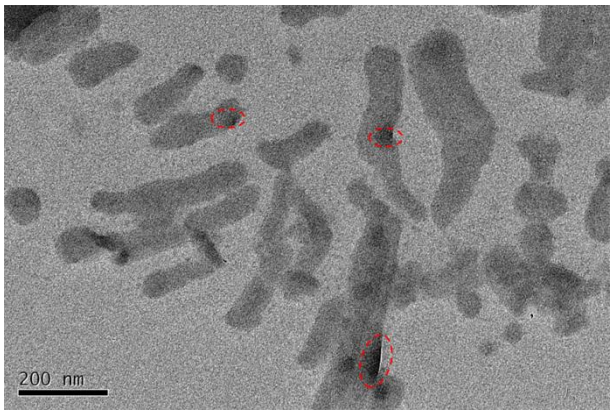

Fig. S6 TEM images of μ-PEG-PS-PDEA$_{9.3k}$ assemblies after CO_2 stimulation. No staining agent was used.

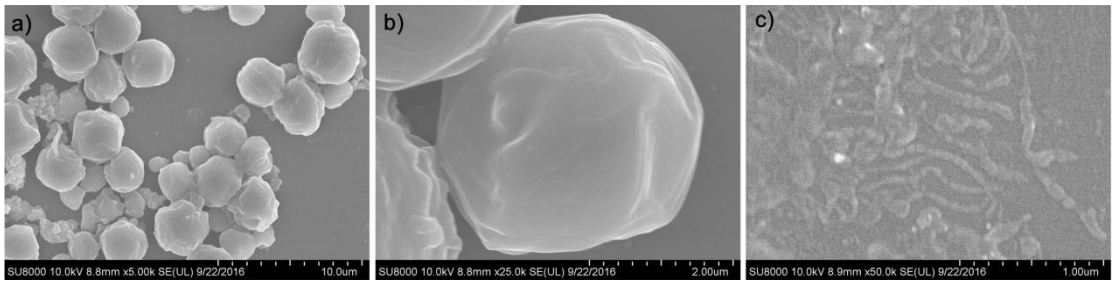

Fig. S7 SEM characterization of μ-PEG-PS-PDEA$_{12.2k}$ a), b) before and c) after CO_2 purging.

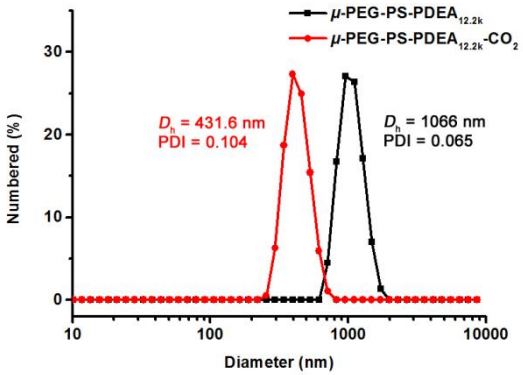

Fig. S8 DLS characterization of μ-PEG-PS-PDEA$_{12.2k}$ before and after CO_2 purging.

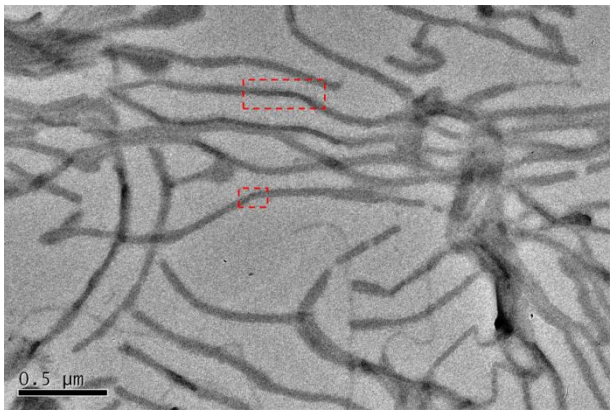

Fig. S9 TEM images of μ-PEG-PS-PDEA$_{12.2k}$ assemblies after CO_2 stimulation. No staining agent was used.

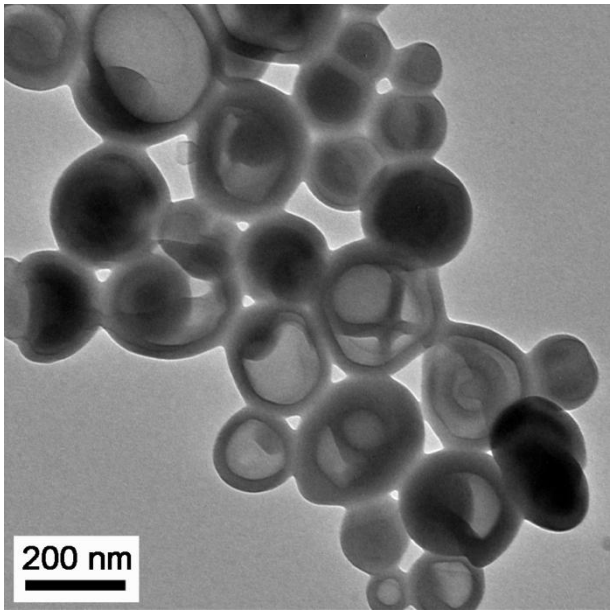

Fig. S10 Small vesicles were observed in the TEM image of μ-PEG-PS-PDEA$_{25k}$ assemblies.

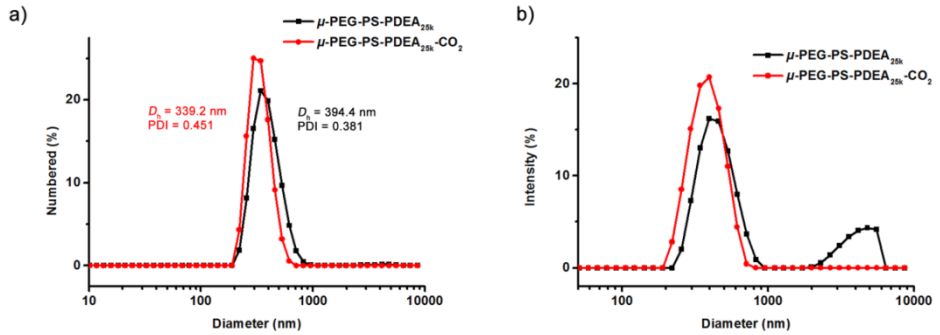

Fig. S11 DLS characterization of μ-PEG-PS-PDEA$_{25k}$ before and after CO_2 purging. a) Number-averaged size distribution. b) Intensity-averaged size distribution.

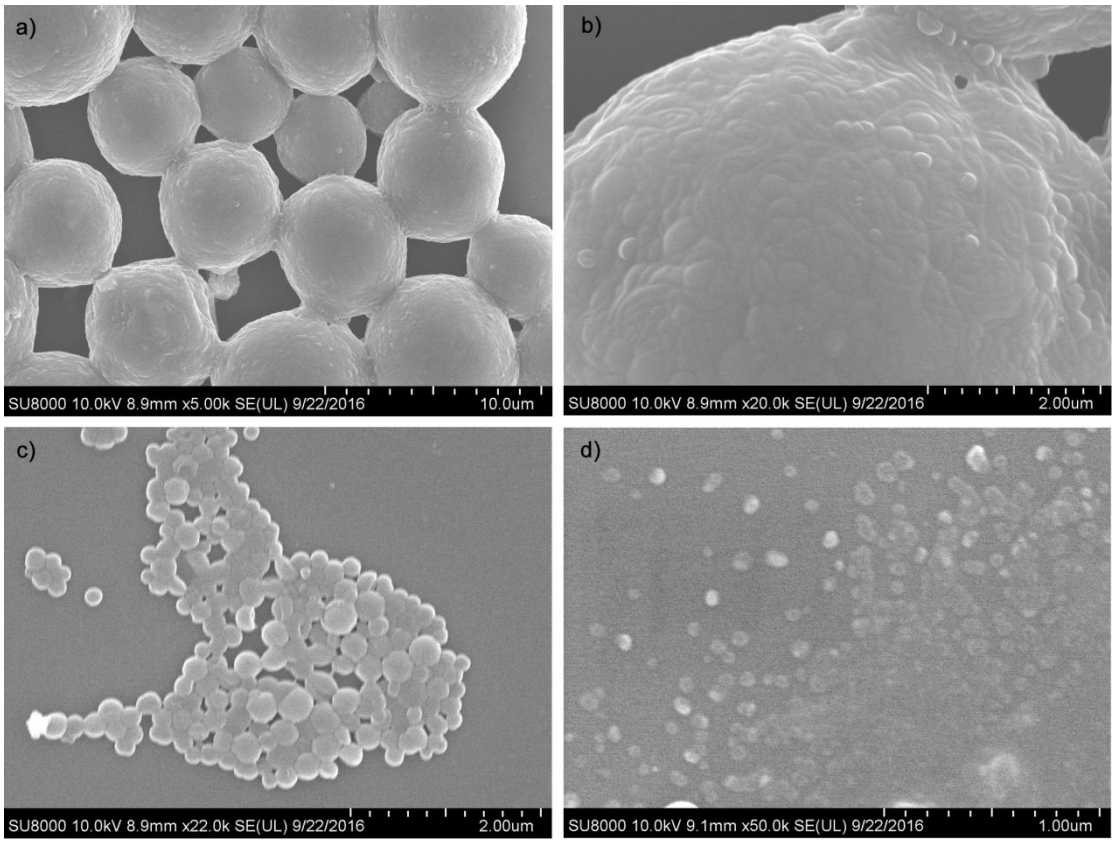

Fig. S12 SEM characterization of μ-PEG-PS-PDEA$_{25k}$ a), b), c) before and d) after CO_2 purging.

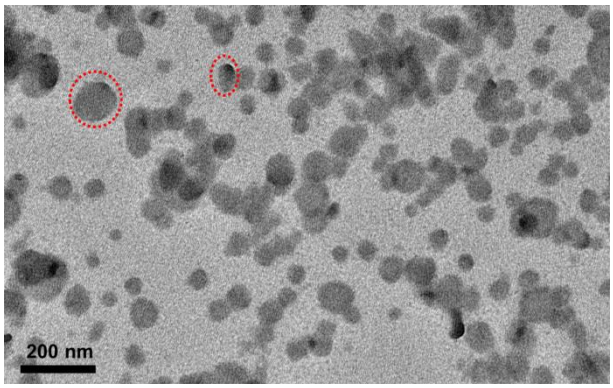

Fig. S13 TEM images of μ-PEG-PS-PDEA$_{25k}$ assemblies after CO_2 stimulation. No staining agent was used.

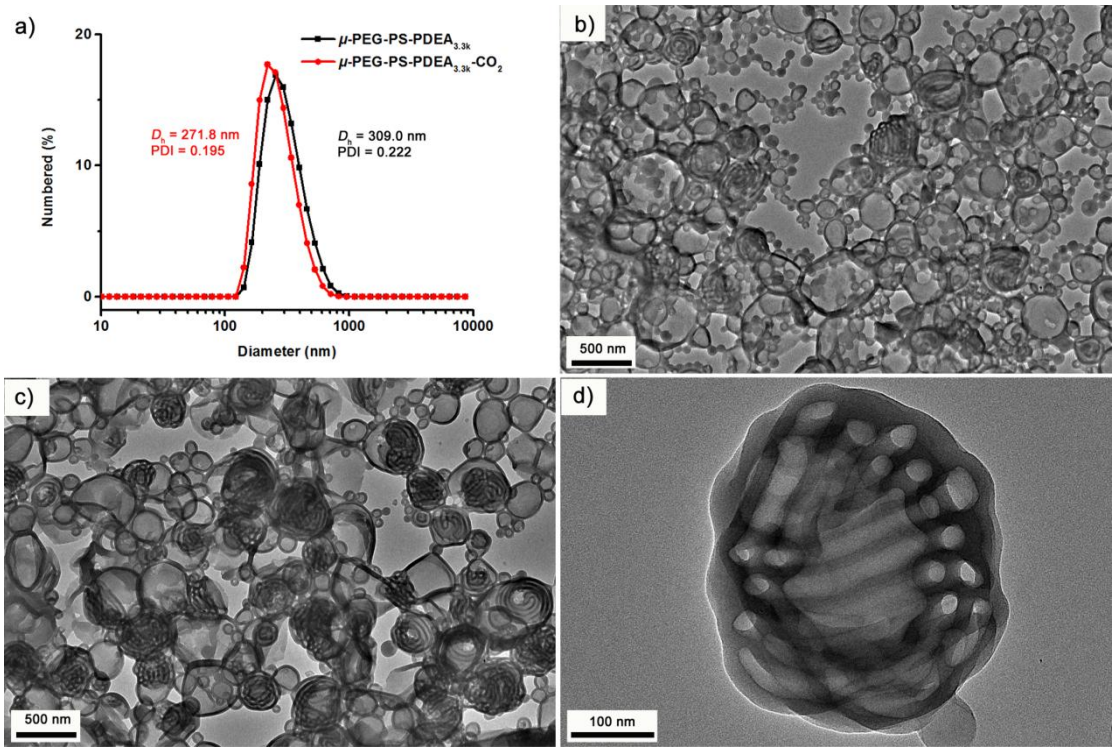

Fig. S14 a) DLS characterization of μ-PEG-PS-PDEA$_{3.3k}$ before and after CO_2 purging. TEM characterization of μ-PEG-PS-PDEA$_{3.3k}$ b) before and c) after CO_2 purging. d) HRTEM image of the HHH structure of μ-PEG-PS-PDEA$_{3.3k}$ assemblies.

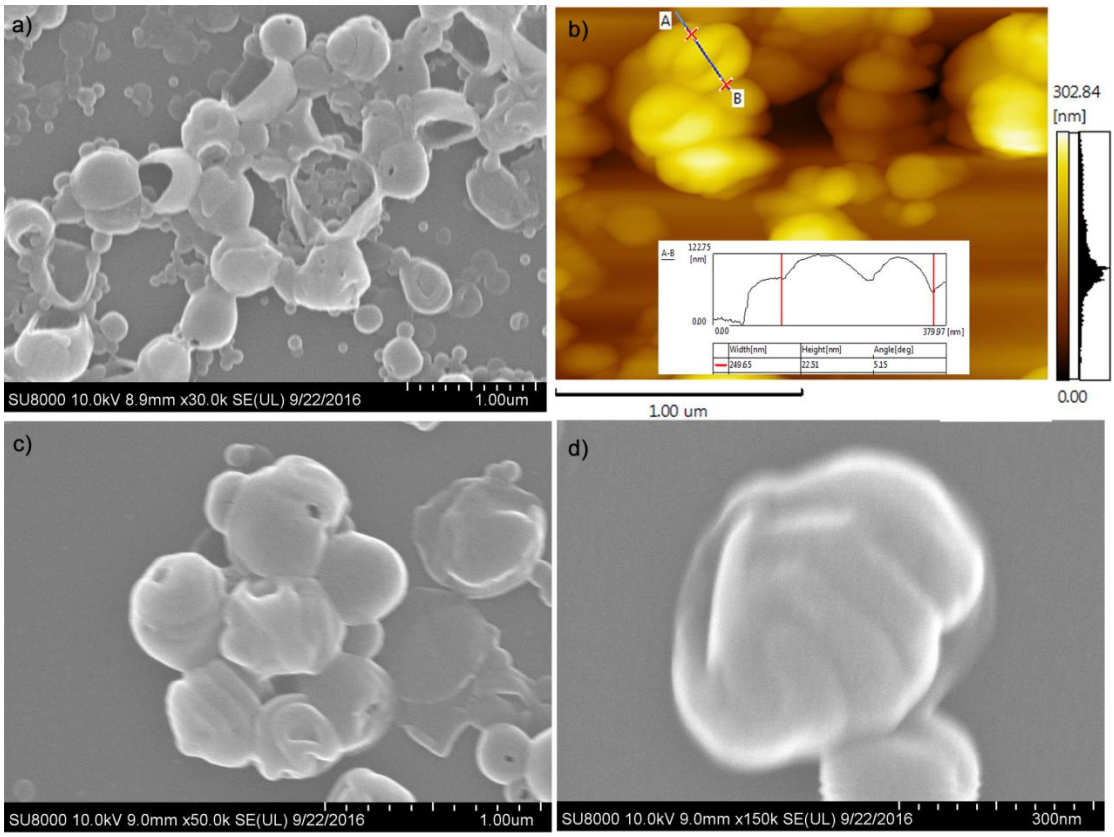

Fig. S15 a) SEM and b) AFM characterization of μ-PEG-PS-PDEA$_{3.3k}$ before CO_2 purging. c), d) SEM characterization of μ-PEG-PS-PDEA$_{3.3k}$ after CO_2 purging.

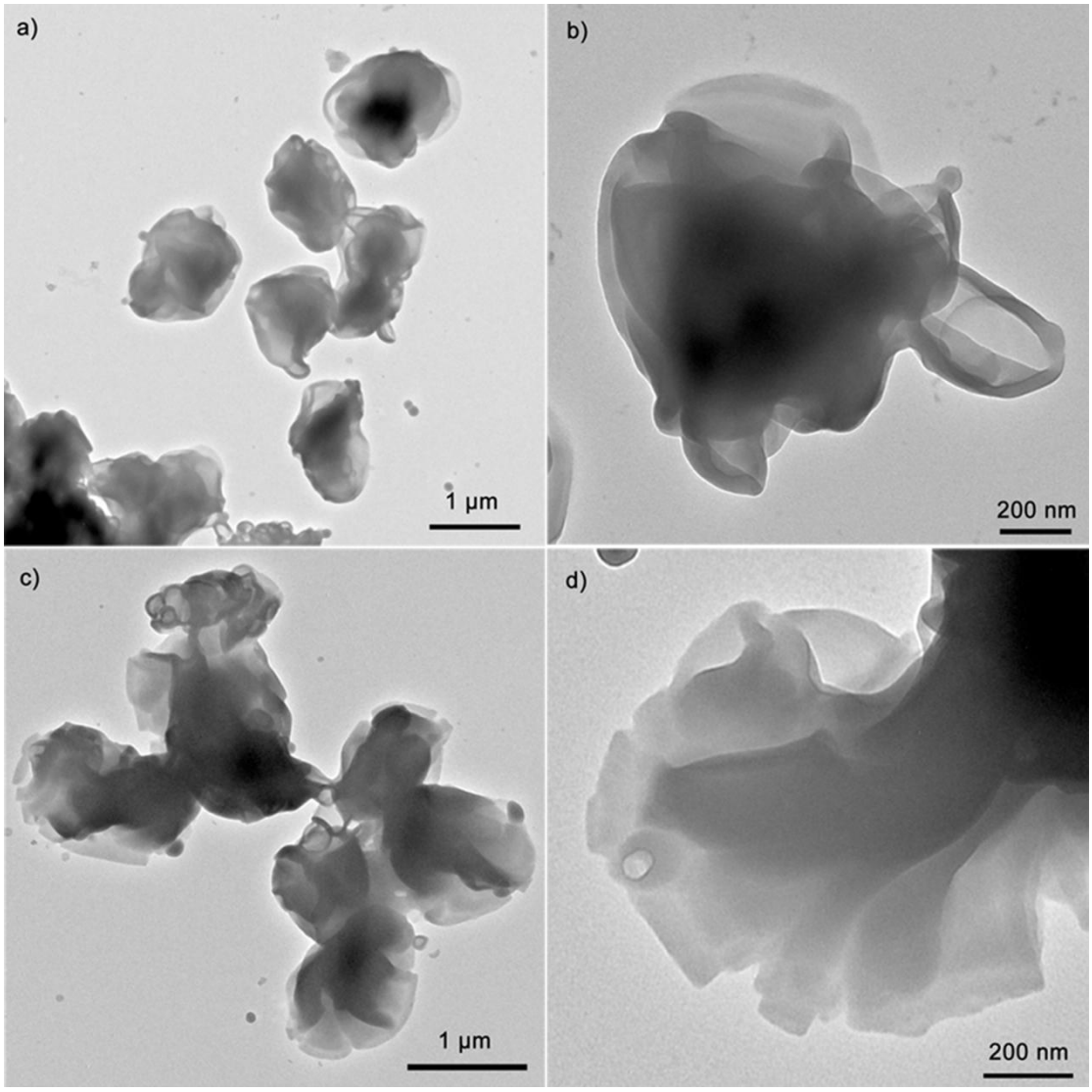

Fig. S16 TEM characterization of μ-PEG-PS-PDEA$_{6.8k}$ a), b) before and c), d) after CO_2 purging.

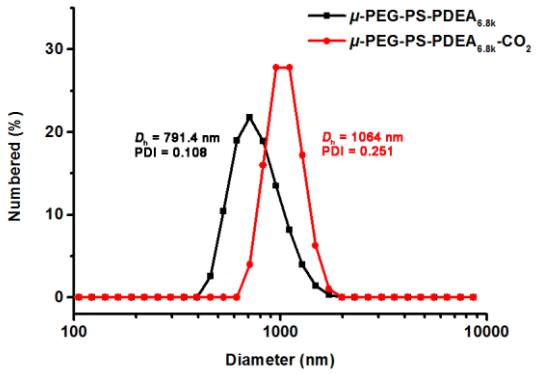

Fig. S17 DLS characterization of μ-PEG-PS-PDEA$_{6.8k}$ before and after CO_2 purging.

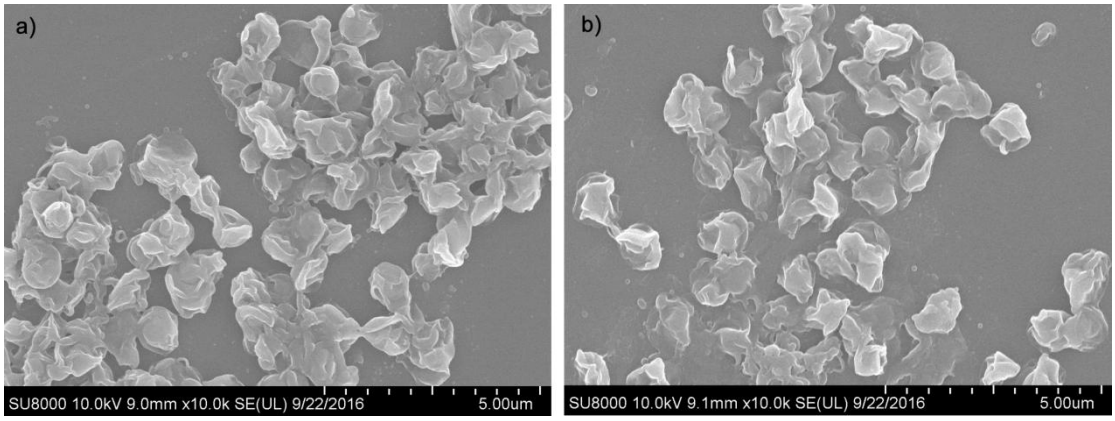

Fig. S18 SEM characterization of μ-PEG-PS-PDEA$_{6.8k}$ a) before and b) after CO_2 purging.

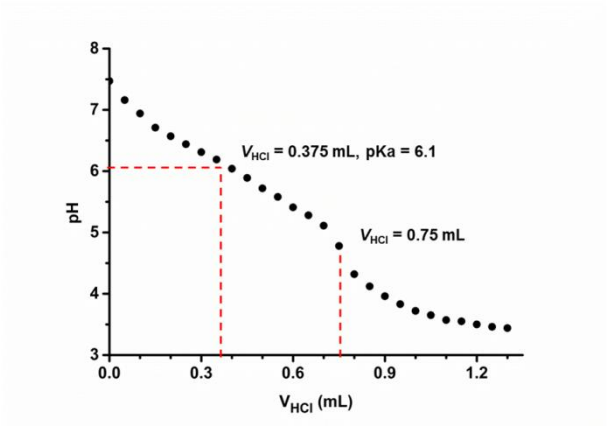

Fig. S19 pH titration curve of the μ-PEG-PS-PDEA$_{6.8k}$ star terpolymer.

Table S1 Zeta potential of μ-PEG-PS-PDEA assemblies before and after CO_2 purging.

Sample	Before CO_2 purging/mV	After CO_2 purging/mV
μ-PEG-PS-PDEA$_{3.3k}$	+45.7	+57.8
μ-PEG-PS-PDEA$_{6.8k}$	+22.7	+34.9
μ-PEG-PS-PDEA$_{9.3k}$	+36.0	+49.4
μ-PEG-PS-PDEA$_{12.2k}$	+62.2	+61.4[a]
μ-PEG-PS-PDEA$_{25k}$	+51.8	+59.7

[a]The zeta potentials were obtained using Malvern Zetasizer Nano ZS90, which measures the electrophoresis mobility and calculates the zeta potential according to the Henry equation ($U_E = \frac{2\varepsilon\zeta}{3\eta} g(\kappa a)$,where U_E is the electrophoretic mobility, ε is the dielectric constant, ζ is the zeta potential, η is the viscosity of the dispersion, and *g(κa)* is the Henry coefficient). However, the classic electrokinetic theory that the commercial instrument adopted ignores the influence of the size and shape of colloids to the electrophoretic mobility. In fact, the size and shape of colloids were found to have significant impacts to the test outcome, where colloids with larger sizes were found to have higher electrophoretic mobility.[S1, S2] As for the CO_2-responsive μ-PEG-PS-PDEA$_{12.2k}$ assemblies, the size of decreased from 1100 nm

to 400 nm after purging with CO_2, and their morphology evolved from sphere to nano-ribbon, which accounts for the inconspicuous zeta potential trend observed.

References

S1. L. Vorwerg, M. Antonietti and K. Tauer, *Colloids Surf., A*, 1999, **150**, 129–135.

S2. M. T. Roy, M. Gallardo and J. Estelrich, *J. Colloid Interface Sci.*, 1998, **206**, 512–517.